Making Sparse Gaussian Elimination Scalable by Static Pivoting

Xiaoye S. Li *
NERSC, Lawrence Berkeley National Lab
1 Cyclotron Rd, MS 50F
Berkeley, CA 94720.
xiaoye@nersc.gov
http://www.nersc.gov/∼xiaoye

James W. Demmel †
Computer Science Division
University of California
Berkeley, CA 94720.
demmel@cs.berkeley.edu
http://www.cs.berkeley.edu/∼demmel

Appeared in the Proceedings of SC 98

Abstract

We propose several techniques as alternatives to partial pivoting to stabilize sparse Gaussian elimination. From numerical experiments we demonstrate that for a wide range of problems the new method is as stable as partial pivoting. The main advantage of the new method over partial pivoting is that it permits *a priori* determination of data structures and communication pattern for Gaussian elimination, which makes it more scalable on distributed memory machines. Based on this *a priori* knowledge, we design highly parallel algorithms for both sparse Gaussian elimination and triangular solve and we show that they are suitable for large-scale distributed memory machines.

Keywords: sparse unsymmetric linear systems, static pivoting, iterative refinement, MPI, 2-D matrix decomposition.

1 Introduction

In our earlier work [8, 9, 22], we developed new algorithms to solve unsymmetric sparse linear systems using Gaussian elimination with partial pivoting (GEPP). The new algorithms are highly efficient on workstations with deep memory hierarchies and shared memory parallel machines with a modest number of processors. The portable implementations of these algorithms appear in the software packages SuperLU (serial) and SuperLU_MT (multithreaded), which are publically available on Netlib [10]. These are among the fastest available codes for this problem.

Our shared memory GEPP algorithm relies on the fine-grained memory access and synchronization that shared memory provides to manage the data structures needed as fill-in is created dynamically, to discover which columns depend on which other columns symbolically, and to use a centralized task queue for scheduling and load balancing. The reason we have to perform all these dynamically is that the computational graph does not unfold until runtime. (This is in contrast to Cholesky, where any pivot order is numerically stable.) However, these techniques are too expensive

*This research used resources of the National Energy Research Scientific Computing Center, which is supported by the Office of Energy Research of the U.S. Department of Energy under Contract No. DE-AC03-76SF00098.

†This research was supported in part by NSF grant ASC-9313958, DOE grant DE-FG03-94ER25219, UT Subcontract No. ORA4466 from ARPA Contract No. DAAL03-91-C0047, DOE grant DE-FG03-94ER25206, NSF Infrastructure grants CDA-8722788 and CDA-9401156 and DOE grant DE-FC03-98ER25351.

(1) Row/column equilibration and row permutation: $A \leftarrow P_r \cdot D_r \cdot A \cdot D_c$,
where D_r and D_c are diagonal matrices and P_r is a row permutation
chosen to make the diagonal large compared to the off-diagonal
(2) Find a column permutation P_c to preserve sparsity: $A \leftarrow P_c \cdot A \cdot P_c^T$
(3) Factorize $A = L \cdot U$ with control of diagonal magnitude
if ($|a_{ii}| < \sqrt{\varepsilon} \cdot ||A||$) **then**
set a_{ii} to $\sqrt{\varepsilon} \cdot ||A||$
endif
(4) Solve $A \cdot x = b$ using the L and U factors, with the following iterative refinement
iterate:
$r = b - A \cdot x$ ... sparse matrix-vector multiply
Solve $A \cdot dx = r$ ... triangular solve
$berr = \max_i \frac{|r|_i}{(|A| \cdot |x| + |b|)_i}$ ... componentwise backward error
if ($berr > \varepsilon$ and $berr \leq \frac{1}{2} \cdot lastberr$) **then**
$x = x + dx$
$lastberr = berr$
goto iterate
endif

Figure 1: The outline of the new GESP algorithm.

on distributed memory machines. Instead, for distributed memory machines, we propose to *not pivot dynamically*, and so enable static data structure optimization, graph manipulation and load balancing (as with Cholesky [20, 25]) and yet *remain numerically stable*. We will retain numerical stability by a variety of techniques: pre-pivoting large elements to the diagonal, iterative refinement, using extra precision when needed, and allowing low rank modifications with corrections at the end. In Section 2 we show the promise of the proposed method from numeric experiments. We call our algorithm GESP for Gaussian elimination with static pivoting. In Section 3, we present an MPI implementation of the distributed algorithms for LU factorization and triangular solve. Both algorithms use an elaborate 2-D (nonuniform) block-cyclic data distribution. Initial results demonstrated good scalability and a factorization rate exceeding 8 Gflops on a 512 node Cray T3E.

2 New algorithm and stability

Traditionally, partial pivoting is used to control the element growth during Gaussian elimination, making the algorithm numerically stable in practice[1]. However partial pivoting is not the only way to control element growth; there are a variety of alternative techniques. In this section we present these alternatives, and show by experiments that appropriate combinations of them can effectively stabilize Gaussian elimination. Furthermore, these techniques are usually inexpensive compared to the overall solution cost, especially for large problems.

2.1 The GESP algorithm

In Figure 1 we sketch our GESP algorithm that incorporates some of the techniques we considered. To motivate step (1), recall that a *diagonally dominant matrix* is one where each diagonal entry a_{ii} is larger in magnitude than the sum of magnitudes of the off-diagonal entries in its row ($\sum_{j \neq i} |a_{ij}|$)

[1]Examples exist where even GEPP is unstable, but these are very rare [7, 19].

or column ($\sum_{j \neq i} |a_{ji}|$). It is known that choosing the diagonal pivots ensures stability for such matrices [7, 19]. So we expect that if each diagonal entry can somehow be made larger relative to the off-diagonals in its row or column, then diagonal pivoting will be more stable. The purpose of step (1) is to choose diagonal matrices D_r and D_c and permutation P_r to make each a_{ii} larger in this sense.

We have experimented with a number of alternative heuristic algorithms for step (1) [13]. All depend on the following graph representation of an $n \times n$ sparse matrix A: it is represented as an undirected weighted bipartite graph with one vertex for each row, one vertex for each column, and an edge with appropriate weight connecting row vertex i to column vertex j for each nonzero entry a_{ij}. Finding a permutation P_r that puts large entries on the diagonal can thus be transformed into a weighted bipartite matching problem on this graph. The diagonal scale matrices D_r and D_r can be chosen independently, to make each row and each column of $D_r A D_c$ have largest entries equal to 1 in magnitude (using the algorithm in LAPACK subroutine DGEEQU [3]). Then there are algorithms in [13] that choose P_r to maximize different properties of the diagonal of $P_r D_r A D_c$, such as the smallest magnitude of any diagonal entry, or the sum or product of magnitudes. But the best algorithm in practice seems to be the one in [13] that picks P_r, D_r and D_c simultaneously so that each diagonal entry of $P_r D_r A D_c$ is ± 1, each off-diagonal entry is bounded by 1 in magnitude, and the product of the diagonal entries is maximized. We will report results for this algorithm only. The worst case serial complexity of this algorithm is $O(n \cdot nnz(A) \cdot \log n)$, where $nnz(A)$ is the number of nonzeros in A. In practice it is much faster; actual timings appear later.

Step (2) is not new and is needed in both SuperLU and SuperLU_MT [10]. The column permutation P_c can be obtained from any fill-reducing heuristic. For now, we use the minimum degree ordering algorithm [23] on the structure of $A^T A$. In the future, we will use the approximate minimum degree column ordering algorithm by Davis *et. al.* [6] which is faster and requires less memory since it does not explicitly form $A^T A$. We can also use nested dissection on $A + A^T$ or $A^T A$ [17]. Note that we also apply P_c to the rows of A to ensure that the large diagonal entries obtained from Step (1) remain on the diagonal.

In step (3), we simply set any tiny pivots encountered during elimination to $\sqrt{\varepsilon} \cdot \|A\|$, where ε is machine precision. This is equivalent to a small (half precision) perturbation to the original problem, and trades off some numerical stability for the ability to keep pivots from getting too small.

In step (4), we perform a few steps of iterative refinement if the solution is not accurate enough, which also corrects for the $\sqrt{\varepsilon} \cdot \|A\|$ perturbations in step (3). The termination criterion is based on the componentwise backward error *berr* [7]. The condition $berr \leq \varepsilon$ means that the computed solution is the exact solution of a slightly different sparse linear system $(A + \delta A)x = b$ where each *nonzero* entry a_{ij} has been changed by at most one unit in its last place, and the zero entries are left unchanged; thus one can say that the answer is as accurate as the data deserves. We terminate the iteration when the backward error *berr* is smaller than machine epsilon, or when it does not decrease by at least a factor of two compared with the previous iteration. The second test is to avoid possible stagnation. (Figure 5 shows that *berr* is always small.)

2.2 Numerical results

In this subsection, we illustrate the numerical stability and runtime of our GESP algorithm on 53 unsymmetric matrices from a wide variety of applications. The application domains of the matrices are given in Table 1. Most of them, except for two (ECL32, WU), can be obtained from the Harwell-Boeing Collection [14] and the collection of Davis [5]. Matrix ECL32 was provided by Jagesh Sanghavi from EECS Department of UC Berkeley. Matrix WU was provided by Yushu

Discipline	Matrices
fluid flow, CFD	af23560, bbmat, bramley1, bramley2, ex11, fidapm11, garon2, graham1, lnsp3937, lns_3937, raefsky3, rma10, venkat01, wu
fluid mechanics	goodwin, rim
circuit simulation	add32, gre_1107, jpwh_991, memplus, onetone1, onetone2, twotone
device simulation	wang3, wang4, ecl32
chemical engineering	extr1, hydr1, lhr01, radfr1, rdist1, rdist2, rdist3a, west2021
petroleum engineering	orsirr_1, orsreg_1, sherman3, sherman4, sherman5
finite element PDE	av4408, av11924
stiff ODE	fs_541_2
Olmstead flow model	olm5000
aeroelasticity	tols4000
reservoir modelling	pores_2
crystal growth simulation	cry10000
power flow modelling	gemat11
dielectric waveguide	dw8192 (eigenproblem)
astrophysics	mcfe
plasma physics	utm5940
demography	psmigr_1
economics	mahindas, orani678

Table 1: Test matrices and their disciplines.

Wu from Earth Sciences Division of Lawrence Berkeley National Laboratory. Figure 2 plots the dimension, $nnz(A)$, and $nnz(L+U)$, i.e. the number of nonzeros in the L and U factors (the *fill-in*). The matrices are sorted in increasing order of the factorization time. The matrices of most interest for parallelization are the ones that take the most time, i.e. the ones on the right of this graph. From the figure it is clear that the matrices large in dimension and number of nonzeros also require more time to factorize. The timing results reported in this subsection are obtained on an SGI ONYX2 machine running IRIX 6.4. The system has 8 195 MHz MIPS R10000 processors and 5120 Mbytes main memory. We only use a single processor, since we are mainly interested in numerical accuracy. Parallel runtimes are reported in section 3.

Detailed performance results from this section in tabular format are available at http://www.nersc.gov/∼xiaoye/SC98/.

Among the 53 matrices, most would get wrong answers or fail completely (via division by a zero pivot) without any pivoting or other precautions. 22 matrices contain zeros on the diagonal to begin with which remain zero during elimination, and 5 more create zeros on the diagonal during elimination. Therefore, not pivoting at all would fail completely on these 27 matrices. Most of the other 26 matrices would get unacceptably large errors due to pivot growth. For our experiment, the right-hand side vector is generated so that the true solution x_{true} is a vector of all ones. IEEE double precision is used as the working precision, with machine epsilon $\approx 10^{-16}$. Figure 3 shows the number of iterations taken in the iterative refinement step. Most matrices terminate the iteration with no more than 3 steps. 5 matrices require 1 step, 31 matrices require 2 steps, 9 matrices require 3 steps, and 8 matrices require more than 3 steps. For each matrix, we present two error metrics, in Figure 4 and Figure 5, to assess the accuracy and stability of GESP. Figure 4 plots the error from GESP versus the error from GEPP (as implemented in SuperLU) for each matrix: A red dot on the green diagonal means the two errors were the same, a red dot below the diagonal means

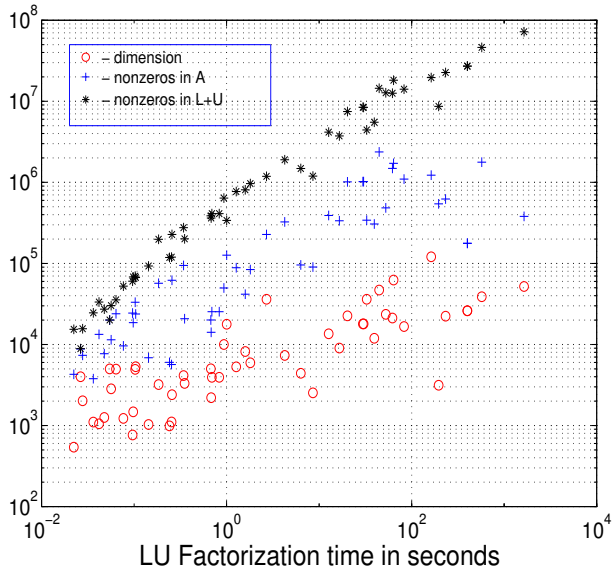

Figure 2: Characteristics of the matrices.

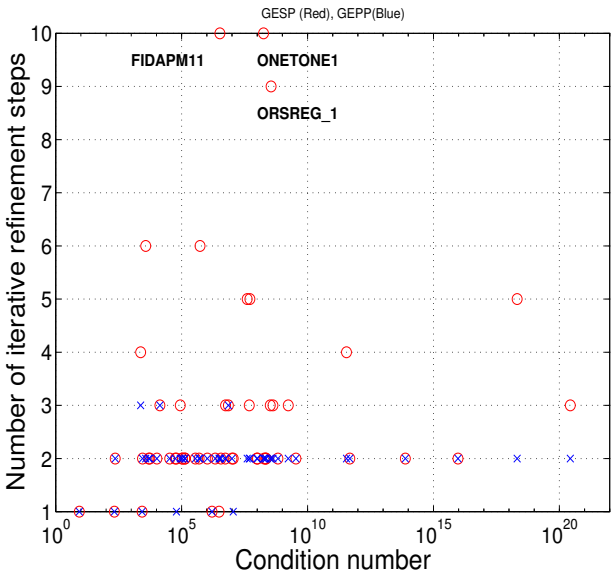

Figure 3: Iterative refinement steps in GESP.

GESP is more accurate, and a red dot above means GEPP is more accurate. Figure 4 shows that the error of GESP is at most a little larger, and can be smaller (21 out of 53), than the error from GEPP. Figure 5 shows that the componentwise backward error [7] is also small, usually near machine epsilon, and never larger than 10^{-12}.

Although the combination of the techniques in steps (1) and (3) in Figure 1 works well for most matrices, we found a few matrices for which other combinations are better. For example, for FIDAPM11, JPWH_991 and ORSIRR_1, the errors are large unless we omit P_r from step (1). For EX11 and RADRF1, we cannot replace tiny pivots by $\sqrt{\varepsilon} \cdot ||A||$ (in step (3)). Therefore, in the software, we provide a flexible interface so the user is able to turn on or off any of these options.

We now evaluate the cost of each step in GESP Figure 1. This is done with respect to the serial implementation, since we have only parallelized the numerical phases of the algorithm (steps (3) and (4)), which are the most time-consuming. In particular, for large enough matrices, the LU factorization in step (3) dominates all the other steps, so we will measure the times of each step with respect to step (3).

Simple equilibration in step (1) (computing D_r and D_c using the algorithm in DGEEQU from LAPACK) is usually negligible and is easy to parallelize. Both row and column permutation algorithms in steps (1) and (2) (computing P_r and P_c) are not easy to parallelize (their parallelization is future work). Fortunately, their memory requirement is just $O(nnz(A))$ [6, 13], whereas the memory requirement for L and U factors grows superlinearly in $nnz(A)$, so in the meantime we can run them on a single processor.

Figure 6 shows the fraction of time spent finding P_r in step (1) using the algorithm in [13], as a fraction of the factorization time. The time is significant for small problems, but drops to 1% to 10% for large matrices requiring a long time to factor, the problems of most interest on parallel machines.

The time to find a sparsity-preserving ordering P_c in step (2) is very much matrix dependent. It is usually cheaper than factorization, although there exist matrices for which the ordering is more expensive. Nevertheless, in applications where we repeatedly solve a system of equations with the same nonzero pattern but different values, the ordering algorithm needs to be run only once, and its cost can be amortized over all the factorizations. We plan to replace this part of the algorithm

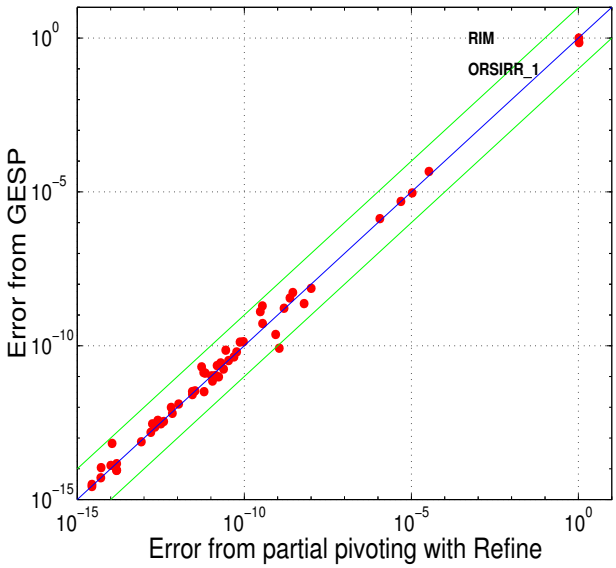

Figure 4: The error $\frac{||x_{true}-x||_\infty}{||x||_\infty}$.

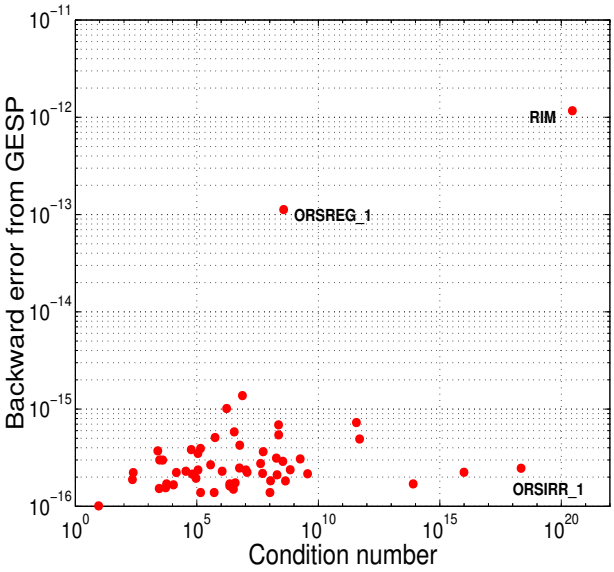

Figure 5: The backward error $\max_i \frac{|A\cdot x-b|_i}{(|A|\cdot|x|+|b|)_i}$.

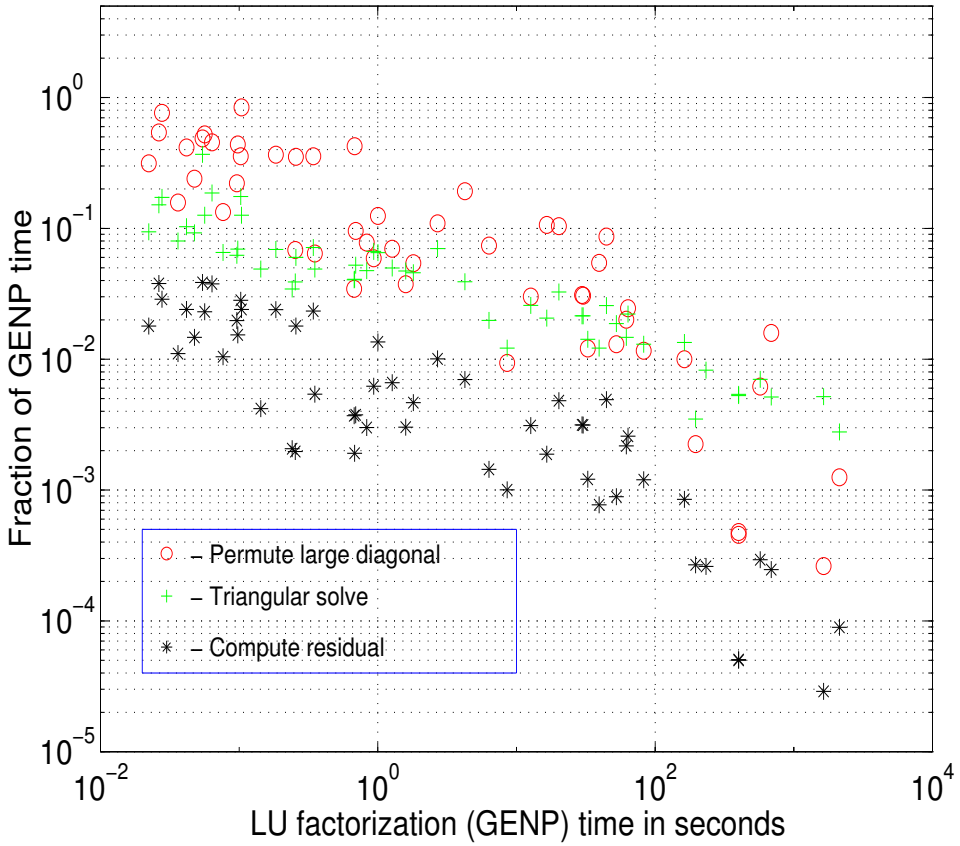

Figure 6: The times to factorize, solve, permute large diagonal, compute residual and estimate error bound, on a 195 MHz MIPS R10000.

	Order	$nnz(A)$	NumSym	StrSym	$nnz(L+U-I)$ ($\times 10^6$)	Flops ($\times 10^9$)
AF23560	23560	460598	.0512	.9465	12.8	4.9
BBMAT	38744	1771722	.0224	.5398	49.1	4.3
ECL32	51993	380415	.6572	.9325	73.5	120.4
EX11	16614	1096948	.9999	1.0000	14.1	8.4
FIDAPM11	22294	623554	.5476	.9965	23.0	17.9
RMA10	46835	2374001	.2443	.9809	14.7	1.8
TWOTONE	120750	1224224	.1418	.2738	22.6	8.7
WANG4	26068	177196	.1868	1.0000	27.7	35.3

Table 2: Characteristics of the test matrices. NumSym is the fraction of nonzeros matched by equal values in symmetric locations. StrSym is the fraction of nonzeros matched by nonzeros in symmetric locations.

with something faster, as outlined in Section 2.1.

As can be seen in Figure 6, computing the residual (sparse matrix-vector multiplication $r = b - A \cdot x$) is cheaper than a triangular solve ($A \cdot dx = r$), and both take a small fraction of the factorization time. For large matrices the solve time is often less than 5% of the factorization time. Both algorithms have been parallelized (see section 3 for parallel performance data).

Finally, our code has the ability to estimate a forward error bound for the true error $\frac{||x_{true}-x||_\infty}{||x||_\infty}$. This is by far the most expensive step after factorization. (For small matrices, it can be more expensive than factorization, since it requires multiple triangular solves.) Therefore, we will do this only when the user asks for it.

3 An implementation with MPI

In this section, we describe our design, implementation and the performance of the distributed algorithms for two main steps of the GESP method, sparse LU factorization (step (3)) and sparse triangular solve (used in step (4)). Our implementation uses MPI [26] to communicate data, and so is highly portable. We have tested the code on a number of platforms, such as Cray T3E, IBM SP2, and Berkeley NOW. Here, we only report the results from a 512 node Cray T3E-900 at NERSC. To illustrate scalability of the algorithms, we restrict our attention to eight relatively large matrices selected from our testbed in Table 1. They are representative of different application domains. The characteristics of these matrices are given in Table 2.

3.1 Matrix distribution and distributed data structure

We distribute the matrix in a two-dimensional block-cyclic fashion. In this distribution, the P processes (not restricted to be a power of 2) are arranged as a 2-D process grid of shape $P_r \times P_c$. The matrix is decomposed into blocks of submatrices. Then, these blocks are cyclically mapped onto the process grid, in both row and column dimensions. Although a 1-D decomposition is more natural to sparse matrices and is much easier to implement, a 2-D layout strikes a good balance among locality (by blocking), load balance (by cyclic mapping), and lower communication volume (by 2-D mapping). 2-D layouts were used in scalable implementations of sparse Cholesky factorization [20, 25].

We now describe how we partition a global matrix into blocks. Our partitioning is based on the notion of *unsymmetric supernode* first introduced in [8]. Let L be the lower triangular matrix in the LU factorization. A supernode is a range $(r : s)$ of columns of L with the triangular block just below the diagonal being full, and with the same row structure below this block. Because of the identical row structure of a supernode, it can be stored in a dense format in memory. This supernode partition is used as our block partition in both row and column dimensions. If there are N supernodes in an n-by-n matrix, the matrix will be partitioned into N^2 blocks of nonuniform size. The size of each block is matrix dependent. It should be clear that all the diagonal blocks are square and full (we store zeros from U in the upper triangle of the diagonal block), whereas the off-diagonal blocks may be rectangular and may not be full. The matrix in Figure 7 illustrates such a partitioning. By block-cyclic mapping we mean block (I, J) $(0 \leq I, J \leq N-1)$ is mapped onto the process at coordinate (I mod P_r, J mod P_c) of the process grid. Using this mapping, a block $L(I, J)$ in the factorization is only needed by the row of processes that own blocks in row I. Similarly, a block $U(I, J)$ is only needed by the column of processes that own blocks in column J.

In this 2-D mapping, each block column of L resides on more than one process, namely, a column of processes. For example in Figure 7, the k-th block column of L resides on the column processes {0, 3}. Process 3 only owns two nonzero blocks, which are not contiguous in the global matrix. The schema on the right of Figure 7 depicts the data structure to store the nonzero blocks on a process. Besides the numerical values stored in a Fortran-style array `nzval[]` in column major order, we need the information to interpret the location and row subscript of each nonzero. This is stored in an integer array `index[]`, which includes the information for the whole block column and for each individual block in it. Note that many off-diagonal blocks are zero and hence not stored. Neither do we store the zeros in a nonzero block. Both lower and upper triangles of the diagonal block are stored in the L data structure. A process owns $\lceil N/P_c \rceil$ block columns of L, so it needs $\lceil N/P_c \rceil$ pairs of `index/nzval` arrays.

For matrix U, we use a row oriented storage for the block rows owned by a process, although for the numerical values within each block we still use column major order. Similarly to L, we also use a pair of `index/nzval` arrays to store a block row of U. Due to asymmetry, each nonzero block in U has the skyline structure as shown in Figure 7 (see [8] for details on the skyline structure). Therefore, the organization of the `index[]` array is different from that for L, which we omit showing in the figure.

Since we do no dynamic pivoting, the nonzero patterns of L and U can be determined during symbolic factorization before numerical factorization begins. Therefore, the block partitioning and the setup of the data structure can all be performed in the symbolic algorithm. This is much cheaper to execute as opposed to partial pivoting where the size of the data structure cannot be forecast and must be determined on the fly as factorization proceeds.

3.2 Sparse LU factorization

Figure 8 outlines the parallel sparse LU factorization algorithm. We use Matlab notation for integer ranges and submatrices. There are three steps in the K-th iteration of the loop. In step (1), only a column of processes participate in factoring the block column $L(K : N, K)$. In step (2), only a row of processes participate in the triangular solves to obtain the block row $U(K, K+1 : N)$. The rank-b update by $L(K+1 : N, K)$ and $U(K, K+1 : N)$ in step (3) represents most of the work and also exhibits more parallelism than the other two steps, where b is the block size of the K-th block column/row. For ease of understanding, the algorithm presented here is simplified. The actual implementation uses a *pipelined* organization so that processes $PROC_C(K+1)$ will start step (1) of iteration $K+1$ as soon as the rank-b update (step (3)) of iteration K to block column

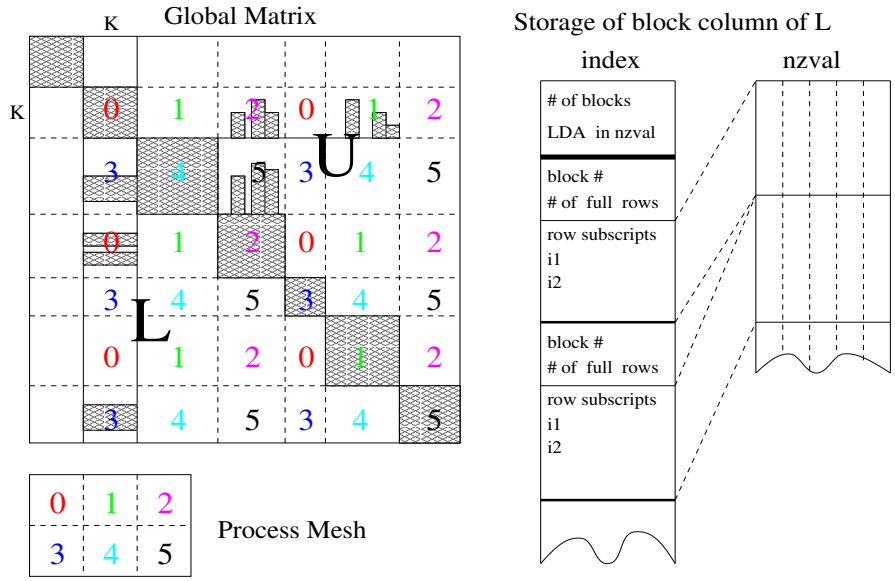

Figure 7: The 2-D block-cyclic layout and the data structure to store a local block column of L.

Let $mycol$ ($myrow$) be my process column (row) number in the process grid
Let $PROC_C(K)$ ($PROC_R(K)$) be the column (row) processes that own block column (row) K
for block $K = 1$ **to** N **do**
(1) **if** ($mycol = PROC_C(K)$)
Obtain the block column factor $L(K:N, K)$
Send $L(K:N, K)$ to the processes in my row who need it
else
Receive $L(K:N, K)$ from processes $PROC_C(K)$ if I need it
endif
(2) **if** ($myrow = PROC_R(K)$)
Perform parallel triangular solves : $U(K, K+1:N) = L(K, K)^{-1} \cdot A(K, K+1:N)$
Send $U(K, K+1:N)$ to processes in my column who need it
else
Receive $U(K, K+1:N)$ from processes $PROC_R(K)$ if I need it
endif
(3) **for** $J = K+1$ to N **do**
for $I = K+1$ to N **do**
if ($myrow = PROC_R(I)$ & $mycol = PROC_C(J)$ & $L(I, K) \neq 0$ & $U(K, J) \neq 0$)
$A(I, J) = A(I, J) - L(I, K) \cdot U(K, J)$
endif
end for

Figure 8: Distributed sparse LU factorization algorithm.

$K+1$ finishes, before completing the update to the trailing matrix $A(K+1:N, K+2:N)$ owned by $PROC_C(K+1)$. The pipelining alleviates the lack of parallelism in both steps (1) and (2). On 64 processors of Cray T3E, for instance, we observed speedups between 10% to 40% over the non-pipelined implementation.

In each iteration, the major communication steps are send/receive $L(K:N, K)$ across process rows and send/receive $U(K, K+1:N)$ down process columns. Our data structure (see Figure 7) ensures that all the blocks of $L(K:N, K)$ and $U(K, K+1:N)$ on a process are contiguous in memory, thereby eliminating the need for packing and unpacking in a send-receive operation or sending many more smaller messages. In each send-receive pair, two messages are exchanged, one for `index[]` and another for `nzval[]`. To further reduce the amount of communication, we employ the notion of *elimination dags* (EDAGs) [18]. That is, we send the K-th column of L rowwise to the process owning the J-th column of L only if there exists a path between (super)nodes K and J in the elimination dags. This is done similarly for the columnwise communication of rows of U. Therefore, each block in L may be sent to fewer than P_c processes and each block in U may be sent to fewer than P_r processes. In other words, our communication takes into account the sparsity of the factors as opposed to "send-to-all" approach in a dense factorization. For example, for AF23560 on 32 (4×8) processes, the total number of messages is reduced from 351052 to 302570, or 16% fewer messages. The reduction is even more with more processes or sparser problems.

3.3 Sparse triangular solve

The sparse lower and upper triangular solves are also designed around the same distributed data structure. The forward substitution proceeds from the bottom of the elimination tree to the root, whereas the back substitution proceeds from the root to the bottom. Figure 9 outlines the algorithm for sparse lower triangular solve. The algorithm is based on a sequential variant called "inner product" formulation. In this formulation, before the K-th subvector $x(K)$ is solved, the update from the inner product of $L(K, 1:K-1)$ and $x(1:K-1)$ must be accumulated and subtracted from $b(K)$. The diagonal process, at the coordinate (K mod P_r, K mod P_c) of the process grid, is responsible for solving $x(K)$. Two counters, $frecv$ and $fmod$, are used to facilitate the asynchronous execution of different operations. $frecv[K]$ counts the number of process updates to $x(K)$ to be received by the diagonal process owning $x(K)$. This is needed because $L(K, 1:K-1)$ is distributed among the row processes $PROC_R(K)$, and due to sparsity, not all processes in $PROC_R(K)$ contribute to the update. When $frecv(K)$ becomes zero, all the necessary updates to $x(K)$ are complete and $x(K)$ is solved. $fmod(K)$ counts the number of block modifications to be summed into the local inner product update (stored in $lsum(K)$) to $x(K)$. When $fmod(K)$ becomes zero, the partial sum $lsum(K)$ is sent to the diagonal process that owns $x(K)$.

The execution of the program is *message-driven*. A process may receive two types of messages, one is the partial sum $lsum(K)$, another is the solution subvector $x(K)$. Appropriate action is taken according to the message type. The asynchronous communication enables large overlapping between communication and computation. This is very important because the communication to computation ratio is much higher in triangular solve than in factorization.

The algorithm for the upper triangular solve is similar to that illustrated in Figure 9. However, because of the row oriented storage scheme used for matrix U, there is a slight complication in the actual implementation. Namely, we have to build two vertical linked lists to enable rapid access of the matrix entries in a block column of U.

Let *mycol* (*myrow*) be my process column (row) number in the process grid
Let $PROC_C(K)$ be the column processes that own block column K
$x = b$
$lsum = 0$
for each block K that I own ... Compute leaf nodes
  if ($myrow = K$ mod P_r & $mycol = K$ mod P_c & $frecv[K] = 0$)
    $x(K) = L(K,K)^{-1} \cdot x(K)$
    Send $x(K)$ to the column processes $PROC_C(K)$
  endif
end for
while (I have more work) **do** ... Compute internal nodes
  Receive a message (*)
  if (message is $lsum(K)$)
    $x(K) = x(K) + lsum(K)$;
    $frecv(K) = frecv(K) - 1$
    if ($frecv(K) = 0$)
      $x(K) = L(K,K)^{-1} \cdot x(K)$
      Send $x(K)$ to the column processes $PROC_C(K)$
    endif
  else if (message is $x(K)$)
    for each $I > K$, $L(I,K) \neq 0$ that I own
      $lsum(I) = lsum(I) - L(I,K) \cdot x(K)$
      $fmod(I) = fmod(I) - 1$
      if ($fmod(I) = 0$)
        Send $lsum(I)$ to the diagonal process who owns $L(I,I)$
      endif
    end for
  endif
end while

Figure 9: Distributed lower triangular solve $L \cdot x = b$.

	Symbolic	Numeric							
		P=4	16	32	64	128	256	512	Mflops
AF23560	1.69	32.26	11.05	7.33	5.94	**5.88**	7.08	7.16	856
BBMAT	11.81	636.52	163.48	92.72	52.07	32.10	22.85	**18.52**	2493
ECL32	14.02	462.74	123.95	68.55	37.47	23.33	17.50	**14.97**	8352
EX11	1.77	27.45	8.80	5.35	3.81	**3.19**	3.47	3.39	2628
FIDAPM11	4.10	162.37	45.33	26.53	15.55	10.22	8.34	**7.85**	2291
RMA10	1.67	21.20	9.36	7.00	6.86	**6.49**	7.58	7.47	511
TWOTONE	6.61	152.27	70.22	42.44	33.36	31.46	**29.96**	31.72	297
WANG4	4.28	104.73	29.71	16.45	10.19	7.13	7.11	**6.59**	5542

Table 3: LU factorization time in seconds and Megaflop rate on the 512 node T3E-900.

3.4 Parallel performance

Recall that we partition the blocks based on supernodes, so the largest block size equals the number of columns of the largest supernode. For large matrices, this can be a few thousand, especially towards the end of matrix L. Such a large granularity would lead to very poor parallelism and load balance. Therefore, when this occurs, we break the large supernode into smaller chunks, so that each chunk does not exceed our preset threshold, the maximum block size. By experimenting, we found that a maximum block size between 20 and 30 is good on the Cray T3E. We used 24 for all the performance results reported in this section.

Table 3 shows the performance of the factorization on the Cray T3E-900. The symbolic analysis (steps (1) and (2) in Figure 1) is not yet parallel, so we start with a copy of the entire matrix on each processor, and run steps (1) and (2) independently on each processor. Thus the time is independent of the number of processors. The first column of Table 3 reports the time spent in the symbolic analysis. The memory requirement of the symbolic analysis is small, because we only store and manipulate the *supernodal graph* of L and the *skeleton graph* of U, which are much smaller than the graphs of L and U. The subsequent columns in the table show the factorization time with a varying number of processors. For four large matrices (BBMAT, ECL32, FIDAPM11 and WANG4), the factorization time continues decreasing up to 512 processors, demonstrating good scalability. The last column reports the numeric factorization rate in Mflops. More than 8 Gflops is achieved for matrix ECL32. This is the fastest published result we have seen for any implementation of parallel sparse Gaussian elimination.

Table 3 starts with $P = 4$ processors because some of the examples could not run with fewer processors. As a reference, we compare our distributed memory code to our shared memory SuperLU_MT code using small numbers of processors. For example, using 4 processor DEC AlphaServer 8400 (SMP) [2], the factorization times of SuperLU_MT for matrices AF23560 and EX11 are 19 and 23 seconds, respectively, comparable to the 4 processor T3E timings. This indicates that our distributed data structure and message passing algorithm do not incur much overhead.

Table 4 shows the performance of the lower and upper triangular solves altogether. When the number of processors continues increasing beyond 64, the solve time remains roughly the same. Although triangular solves do not achieve high Megaflop rates, the time is usually much less than that for factorization.

The efficiency of a parallel algorithm depends mainly on how the workload is distributed and how much time is spent in communication. One way to measure load balance is as follows. Let

[2]Each processor is the same as one T3E processor, except there is a 4 MB tertiary cache.

	P=4	8	16	32	64	Mflops
AF23560	0.94	0.90	0.69	0.67	0.64	42
BBMAT	3.69	3.42	2.27	2.23	1.83	56
ECL32	2.95	2.60	1.66	1.57	1.17	128
EX11	0.50	0.46	0.32	0.31	0.26	112
FIDAPM11	1.39	1.26	0.83	0.83	0.68	70
RMA10	0.77	0.74	0.58	0.53	0.50	60
TWOTONE	4.37	4.37	3.65	3.15	2.95	16
WANG4	1.09	0.99	0.67	0.63	0.50	112

Table 4: Triangular solves time in seconds and Megaflop rate on the T3E-900.

	AF23560	BBMAT	ECL32	EX11	FIDAPM11	RMA10	TWOTONE	WANG4
B_{fact}	.82	.77	.94	.87	.70	.73	.43	.92
B_{sol}	.84	.81	.92	.83	.81	.76	.66	.88
Comm								
$fact$	.82	.54	.54	.77	.59	.92	.92	.62
sol	.97	.97	.96	.97	.97	.96	.96	.97

Table 5: Load balance and communication on 64 processors Cray T3E.

f_i denote the number of floating-point operations performed on process i. We compute the load balance factor $B = \frac{\sum_i(f_i)}{P \max_i(f_i)}$. In other words, B is the average workload divided by the maximum workload. It is clear that $0 < B \leq 1$, and higher B indicates better load balance. The parallel runtime is at least the runtime of the slowest process, whose workload is highest. In Table 5 we present the load balance factor B for both factorization and solve phases. As can be seen from the table, the distribution of workload is good for most matrices, except for TWOTONE.

In the same table, we also show the fraction of the runtime spent in communication. The numbers were collected from the performance analysis tool called *Apprentice* on the T3E. The amount of communication is quite excessive. Even for the matrices that scale well, such as BBMAT, ECL32, FIDAPM11 and WANG4, more than 50% of the factorization time is spent in communication. For the solve, which has much smaller amount of computation, communication takes more than 95% of the total time. We expect the percentage of communication will be even higher with more processors, because the total amount of computation is more or less constant.

Although TWOTONE is a relatively large matrix, the factorization does not scale as well as for the other large matrices. One reason is that the present submatrix to process mapping results in very poor load distribution. Another reason is due to long time in communication. When we look further into communication time using *Apprentice*, we found that processes are idle 60% of the time waiting to receive the column block of L sent from a process column on the left (step (1) in Figure 8), and are idle 23% of the time waiting to receive the row block of U sent from a process row from above (step (2) in Figure 8). Clearly, the critical path of the algorithm is in step (1), which must preserve certain precedence relation between iterations. Our pipelining method shortens the critical path to some extent, but we expect the length of the critical path can be further reduced by a more sophisticated DAG (task graph) scheduling. For the solve, we found that processes are idle 73% of the time waiting for a message to arrive (at line (*) in Figure 9). So on each process there is not much work to do but a large amount of communication. These communication bottlenecks also occur for the other matrices, but the problems are not so pronounced as TWOTONE.

Another problem with TWOTONE is that supernode size (or block size) is very small, only 2.4 columns on average. This results in poor uniprocessor performance and low Megaflop rate.

4 Concluding remarks and future work

We propose a number of techniques in place of partial pivoting to stabilize sparse Gaussian elimination. Their effectiveness is demonstrated by numerical experiments. These techniques enable static analysis of the nonzero structure of the factors and the communication pattern. As a result, a more scalable implementation becomes feasible on large-scale distributed memory machines with hundreds of processors. Our preliminary software is being used in a quantum chemistry application at Lawrence Berkeley National Laboratory, where a complex unsymmetric system of order 200,000 has been solved within 2 minutes.

4.1 More techniques for numerical stability

Although the current GESP algorithm is successful for a large number of matrices, it fails to solve one finite element matrix, AV41092, because the pivot growth is still too large with any combination of the current techniques. We plan to investigate other complementary techniques to further stabilize the algorithm. For example, we can use a judicious amount of extra precision to store some matrix entries more accurately, and to perform internal computations more accurately. This facility is available for free on Intel architectures, which performs all arithmetic most efficiently in 80-bit registers, and at modest cost on other machines. The extra precision can be used in both factorization and residual computation.

We can also mix static and partial pivoting by only pivoting within a diagonal block owned by a single processor (or SMP within a cluster of SMPs). This can further enhance stability.

We can use a more aggressive pivot size control strategy in step (4) of the algorithm. That is, instead of setting tiny pivots to $\sqrt{\varepsilon} \cdot ||A||$, we may set it to the largest magnitude of the current column. This incurs a non-trivial amount of rank-1 perturbation to the original matrix. In the end, we use Sherman-Morrison-Woodbury formula [7] to recover the inverse of the original matrix, at the cost of a few more steps of inverse iteration.

It remains to be seen in what circumstances these ideas should be employed in practice. There are also theoretical questions to be answered.

4.2 High performance issues

In order to make the solver entirely scalable, we need to parallelize the symbolic algorithm. In this case, we will start with the matrix initially distributed in some manner. The symbolic algorithm then determines the best layout for the numeric algorithms, and redistributes matrix if necessary. This also requires us to provide a good interface so the user knows how to input the matrix in the distributed manner.

For the *LU* factorization, we will investigate more general functions for matrix-to-process mapping and scheduling of computation and communication by exploiting more knowledge from the EDAGs. This is expected to relax much of the synchrony in the current factorization algorithm, and reduce communication. We also consider switching to a dense factorization, such as the one implemented in ScaLAPACK [4], when the submatrix at the lower right corner becomes sufficiently dense. The uniprocessor performance can also be improved by amalgamating small supernodes into large ones.

To speed up the sparse triangular solve, we may apply some graph coloring heuristic to reduce the number of parallel steps [21]. There are also alternative algorithms other than substitutions, such as those based on partitioned inversion [1] or selective inversion [24]. However, these algorithms usually require preprocessing or different matrix distributions than the one used in our factorization. It is unclear whether the preprocessing and redistribution will offset the benefit offered by these algorithms, and will probably depend on the number of right-hand sides.

5 Related work

Duff and Koster [13] applied the techniques of permuting large entries to the diagonal in both direct and iterative methods. In their direct method using a multifrontal approach, the numeric factorization first proceeds with diagonal pivots as previously chosen by the analysis on the structure of $A + A^T$. If a diagonal entry is not numerically stable, its elimination will be delayed, and a larger frontal matrix will be passed to the later stage. They showed that using the initial permutation, the number of delayed pivots were greatly reduced in factorization. They experimented with some iterative methods such as GMRES, BiCGSTAB and QMR using ILU preconditioners. The convergence rate is substantially improved in many cases when the initial permutation is employed.

Amestoy, Duff and L'Excellent [2] implemented the above multifrontal approach for distributed memory machines. The host performs the fill-reducing ordering, estimates each frontal matrix structure, and statically maps the assembly tree, all based on the symmetric pattern of $A + A^T$, and then sends the information to the other processors. During numerical factorization, each frontal matrix is factorized by a master processor and one or more slave processors. Due to possible delayed pivots, the frontal matrix size may be different than predicted by the analysis phase. So the master processor dynamically determines how many slave processors will be actually used for each frontal matrix. They showed good performance on 32 processors IBM SP2.

MCSPARSE [16] is a parallel unsymmetric linear system solver. The key component in the solver is the reordering step, which transforms the matrix into a bordered block upper triangular form. Their reordering first uses an unsymmetric ordering to put relatively large entries on the diagonal. The algorithm is a modified version of Duff [11, 12]. After this unsymmetric ordering, they use several symmetric permutations, which preserve the diagonal, to order the matrix into the desired form. With large diagonal entries, there is a better chance of obtaining a stable factorization by pivoting only within the diagonal blocks. The number of pivots from the border is thus reduced. Large and medium grain parallelism is then exploited to factor the diagonal blocks and eliminate the bordered blocks. They implemented the parallel factorization algorithm on a 32 processor Cedar, an experimental shared memory machine.

Fu, Jiao and Yang [15] designed a parallel LU factorization algorithm based on the following static information. The sparsity pattern of the Householder QR factorization of A contains the union of all sparsity patterns of the LU factors of A for all possible pivot selections. This has been used to do both memory allocation and computation conservatively (on possibly zero entries), but it can be arbitrarily conservative, particularly for matrices arising from circuit and device simulations. For several matrices that do not incur much overestimation, they showed good factorization speed on 128 processors Cray T3E.

It will be interesting to compare the performance of the different approaches.

6 Acknowledgement

We are grateful to Iain Duff for giving us access to the early version of the Harwell subroutine `MC64`, which permutes large entries to the diagonal.

References

[1] Fernando L. Alvarado, Alex Pothen, and Robert Schreiber. Highly parallel sparse triangular solution. In Alan George, John R. Gilbert, and Joseph W.H. Liu, editors, *Graph theory and sparse matrix computation*, pages 159–190. Springer-Verlag, New York, 1993.

[2] P. R. Amestoy, I. S. Duff, and J.-Y. L'Excellent. Multifrontal parallel distributed symmetric and unsymmetric solvers. Technical Report RAL-TR-98-051, Rutherford Appleton Laboratory, 1998.

[3] E. Anderson, Z. Bai, C. Bischof, J. Demmel, J. Dongarra, J. Du Croz, A. Greenbaum, S. Hammarling, A. McKenney, S. Ostrouchov, and D. Sorensen. *LAPACK Users' Guide, Release 2.0.* SIAM, Philadelphia, 1995. 324 pages.

[4] L. S. Blackford, J. Choi, E. D'Azevedo, J. Demmel, I. Dhillon, J. Dongarra, S. Hammarling, G. Henry, A. Petitet, K. Stanley, D. Walker, and R. C. Whaley. *ScaLAPACK Users' Guide.* SIAM, Philadelphia, 1997. 325 pages.

[5] Timothy A. Davis. University of Florida sparse matrix collection. http://www.cise.ufl.edu/∼davis/sparse.

[6] Timothy A. Davis, John R. Gilbert, Esmond Ng, and Barry Peyton. Approximate minimum degree ordering for unsymmetric matrices. Talk presented at XIII Householder Symposium on Numerical Algebra, June 1996. Journal version in preparation.

[7] James W. Demmel. *Applied Numerical Linear Algebra.* SIAM, Philadelphia, 1997.

[8] James W. Demmel, Stanley C. Eisenstat, John R. Gilbert, Xiaoye S. Li, and Joseph W.H. Liu. A supernodal approach to sparse partial pivoting. Technical Report UCB//CSD-95-883, Computer Science Division, U.C. Berkeley, 1995. To appear in *SIAM J. Matrix Anal. Appl.*

[9] James W. Demmel, John R. Gilbert, and Xiaoye S. Li. An asynchronous parallel supernodal algorithm for sparse gaussian elimination. Technical Report UCB//CSD-97-943, Computer Science Division, U.C. Berkeley, 1997. To appear in *SIAM J. Matrix Anal. Appl.*

[10] James W. Demmel, John R. Gilbert, and Xiaoye S. Li. SuperLU and SuperLU_MT, November 1997. http://www.netlib.org/scalapack/prototype/.

[11] I. S. Duff. Algorithm 575. Permutations for a zero-free diagonal. *ACM Trans. Mathematical Software*, 7:387–390, 1981.

[12] I. S. Duff. On algorithms for obtaining a maximum transversal. *ACM Trans. Mathematical Software*, 7:315–330, 1981.

[13] Iain S. Duff and Jacko Koster. The design and use of algorithms for permuting large entries to the diagonal of sparse matrices. Technical Report RAL-TR-97-059, Rutherford Appleton Laboratory, 1997.

[14] I.S. Duff, R.G. Grimes, and J.G. Lewis. Users' guide for the Harwell-Boeing sparse matrix collection (release 1). Technical Report RAL-92-086, Rutherford Appleton Laboratory, December 1992.

[15] C. Fu, X. Jiao, and T. Yang. Efficient sparse LU factorization with partial pivoting on distributed memory architectures. *IEEE Trans. Parallel and Distributed Systems*, 9(2):109–125, 1998.

[16] K. A. Gallivan, B. A. Marsolf, and H. A. G. Wijshoff. Solving large nonsymmetric sparse linear systems using MCSPARSE. *Parallel Computing*, 22:1291–1333, 1996.

[17] J. George. Nested dissection of a regular finite element mesh. *SIAM J. Numerical Analysis*, 10:345–363, 1973.

[18] John R. Gilbert and Joseph W.H. Liu. Elimination structures for unsymmetric sparse LU factors. *SIAM J. Matrix Anal. Appl.*, 14(2):334–352, April 1993.

[19] G. Golub and C. Van Loan. *Matrix Computations*. Johns Hopkins University Press, Baltimore, MD, Third edition, 1996.

[20] A. Gupta and V. Kumar. Optimally scalable parallel sparse cholesky factorization. In *The 7th SIAM Conference on Parallel Processing for Scientific Computing*, pages 442–447, 1995.

[21] Mark T. Jones and Paul E. Plassmann. Scalable iterative solution of sparse linear systems. *Parallel Computing*, (20):753–773, 1994.

[22] Xiaoye S. Li. Sparse Gaussian elimination on high performance computers. Technical Report UCB//CSD-96-919, Computer Science Division, U.C. Berkeley, September 1996. Ph.D dissertation.

[23] Joseph W.H. Liu. Modification of the minimum degree algorithm by multiple elimination. *ACM Trans. Math. Software*, 11:141–153, 1985.

[24] Padma Raghavan. Efficient parallel sparse triangular solution with selective inversion. Technical Report CS-95-314, Department of Computer Science, University of Tennessee, 1995.

[25] E. E. Rothberg and A. Gupta. An efficient block-oriented approach to parallel sparse cholesky factorization. In *Supercomputing*, pages 503–512, November 1993.

[26] Message Passing Interface (MPI) forum. http://www.mpi-forum.org/.